# Retinal ganglion cells act largely as independent encoders

**S. Nirenberg, S. M. Carcieri, A. L. Jacobs & P. E. Latham**

*Department of Neurobiology, University of California Los Angeles, 10833 Le Conte Avenue, Los Angeles, California 90095-1763, USA*

**Correlated firing among neurons is widespread in the visual system. Neighbouring neurons, in areas from retina to cortex, tend to fire together more often than would be expected by chance. The importance of this correlated firing for encoding visual information is unclear and controversial[1–5]. Here we examine its importance in the retina. We present the retina with natural stimuli and record the responses of its output cells, the ganglion cells. We then use information theoretic techniques to measure the amount of information about the stimuli that can be obtained from the cells under two conditions: when their correlated firing is taken into account, and when their correlated firing is ignored. We find that more than 90% of the information about the stimuli can be obtained from the cells when their correlated firing is ignored. This indicates that ganglion cells act largely independently to encode information, which greatly simplifies the problem of decoding their activity.**

A principal goal in vision research is to understand how visual stimuli are encoded in the activity of the ganglion cells, as these cells provide all the information about the visual world that the brain receives. Several studies have proposed that visual stimuli are encoded in a complex way that depends on correlated activity[5–7]. Such activity has been described in many species, including several mammals (cat[8–10], rabbit[11] and monkey[12]). The proposal is that this activity carries information about visual stimuli that is not present in non-correlated activity[5–7].

If correlated firing carries information, then strategies for understanding how ganglion cells encode visual stimuli must take the correlations into account. This means that the activity of a single ganglion cell cannot be evaluated by itself, but rather must be decoded in the context of the firing patterns of other ganglion cells. If, on the other hand, correlated firing does not carry visual information, then the firing of a ganglion cell can be evaluated independently of other cells.

It has been reported[6,7] that correlated activity can carry information, but the methods used in these reports were indirect. Here we addressed the problem directly using an information theoretic approach. We compared the amount of information that could be obtained from pairs of ganglion pairs when their correlations were taken into account with the amount of information that could be obtained from the pairs when their correlations were ignored. The extent to which information is lost when correlations are ignored is the extent to which correlations are important for encoding information.

We used the isolated mouse retina. The stimuli were natural movies, each 7 s long and repeated 300 times, and the ganglion cell responses were recorded using a multielectrode array. We used an array with closely spaced electrodes (25–100 μm apart) to ensure that we recorded from many pairs of neighbouring ganglion cells, which tend to have overlapping receptive fields and show correlated activity[6,9,11].

The data were screened for pairs of responses that passed two criteria. First, both responses had to be clean of contaminating spikes from other cells. This was tested by computing the autocorrelation function for each response, which gives the firing rate as a function of time relative to each spike. As neurons have a refractory period of approximately 1 ms, the autocorrelation function for a single cell should contain a central peak flanked on either side by zero firing rate for 1 ms. Non-zero firing rates in this 1-ms window reflect contamination from electronic noise or spikes from other cells. Only responses showing less than 2% contamination were used. Second, both responses had to have average firing rates above 0.5 Hz. Typical responses are shown in Fig. 1. The dataset contained 76 cells, with 5–20 cells per retina (six retinas). This gave a total of 498 cell pairs, with 10–190 pairs per retina.

We first determined the degree of correlated activity for each pair (Fig. 2a–c). This was measured as the fraction of correlated spikes produced by the pair above chance, taking into account correlations induced by the stimulus. We called this the excess correlated fraction (ECF; see Methods). The ECFs ranged from −1% to +34% (Fig. 2b), in close agreement with similar measurements reported for other mammalian species (the highest excess fraction is 27% in cat[9] and 28% in rabbit[11]). It is also similar to that found for pairs of cells in cat lateral geniculate nucleus (LGN), in which the highest fraction of correlated spikes is, on average, 28% (ref. 13). We then determined the timescale over which the correlations occurred (Fig. 2c). The range was from $< 1$ ms to 11 ms. This is similar to that observed in cat[9] and rabbit[11], although it extends to slightly shorter values. Similar short timescales ($< 1$ ms) are found in cat LGN[13].

To measure the amount of information the pairs of ganglion cells carried about the stimuli when their correlations were taken into account, we used standard information theoretic techniques. We treated the movie as a series of segments of fixed temporal length, with each segment regarded as a separate stimulus. We presented the movie several hundred times to generate a large set of responses (spike trains) to each segment. This allowed us to estimate the probability of getting a particular pair of responses given a particular movie segment—that is, to estimate $P(r_1, r_2|s)$, where $r_1$ was the response of cell 1, $r_2$ was the response of cell 2 and $s$ was the movie segment. Given these conditional probabilities, we then calculated the amount of information, $I$, between the responses and the stimulus segments, using the standard expression[15]

$$I = -\sum_{r_1,r_2} P(r_1, r_2)\log_2 P(r_1, r_2) + \sum_s P(s)\sum_{r_1,r_2} P(r_1, r_2|s)\log_2 P(r_1, r_2|s) \quad (1)$$

where $P(r_1, r_2) = \Sigma_s P(r_1, r_2|s)P(s)$, and $P(s)$ is the probability that a given stimulus segment $s$ occurred. The numerical method for calculating $I$ followed ref. 16; see Methods.

To assess the role of correlations, we calculated how much

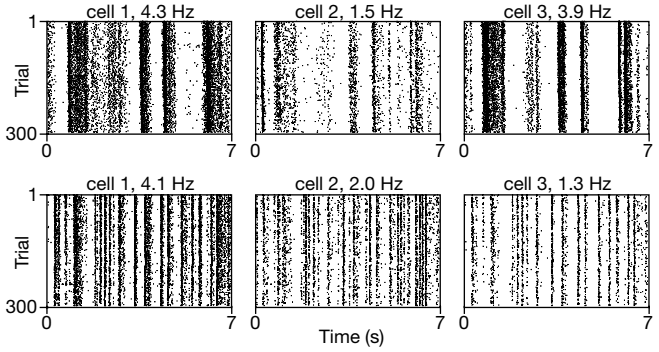


**Figure 1** Typical ganglion cell responses to the movies. Each raster plot shows the response of a ganglion cell to 300 repeats of a movie. The cell's average firing rate during the movie is marked above the plot. Top, responses to Movie 1 (natural scenes); bottom, responses to Movie 3 (spatially uniform, time-varying stimulus). (See Methods for image statistics.) The top and bottom plots in each column are from the same cell.

information would be lost if the correlations in the responses of the two cells were ignored. We 'ignored' the correlations by treating the conditional probability distributions of the two responses, $P(r_1, r_2|s)$, as the product of their individual probability distributions, $P(r_1|s)$ and $P(r_2|s)$. (By definition, two responses are not correlated if their joint probability distribution equals the product of their individual ones.) We denoted this distribution $P_{IND}(r_1,r_2|s)$, with $P_{IND}(r_1, r_2|s) = P(r_1|s)P(r_2|s)$. We then used $P_{IND}(r_1, r_2|s)$ rather than the true distribution, $P(r_1, r_2|s)$, to estimate the probability of a stimulus given a response. As $P_{IND}(r_1, r_2|s)$ is not quite the true distribution, using it should lead to a loss of information. Following a method described in ref. 17 (see Methods), it can be shown that the amount of information lost, denoted $\Delta I$, is given by

$$\Delta I = \sum_s P(s) \sum_{r_1,r_2} P(r_1, r_2|s) \log_2 \left[ \frac{P(r_1, r_2|s)}{P_{IND}(r_1, r_2|s)} \right] - \sum_{r_1,r_2} P(r_1, r_2) \log_2 \left[ \frac{P(r_1, r_2)}{P_{IND}(r_1, r_2)} \right] \quad (2)$$

where $\Delta I$ is in bits, and $P_{IND}(r_1, r_2) = \Sigma_s P(r_1 \mid s)P(r_2 \mid s)P(s)$.

We found that the amount of information lost, $\Delta I$, was remarkably small. Only one pair of cells showed a loss of information of more than 10%. Figure 3 shows the fraction of information lost for each pair, with the fraction plotted against the ECF. Although the fraction of information lost generally increased for pairs with high ECFs, the fraction lost never exceeded 11%. Thus, in the mouse retina, we find that ignoring correlations leads to only a small loss of information. Certainly, if there were pairs of ganglion cells with higher degrees of correlation, above the 34% we observed, a greater loss might be expected; however, in no mammalian species examined is the degree of correlated activity reported to be higher (as mentioned above, the highest reported ECF for cat retinal ganglion cells[9] is 27% and for rabbit[11], 28%).

The loss of information was measured using responses binned at 1 ms to ensure that all information in the correlations, which occur largely on that timescale (Fig. 2c), was captured. The small bins, though, required us to use short responses, so temporal correlations beyond 10 ms were not captured. However, we also measured the loss of information using larger bins (10 ms), to better capture information in the broader correlations, and the same result was obtained: no pair showed a loss of information greater than 11%.

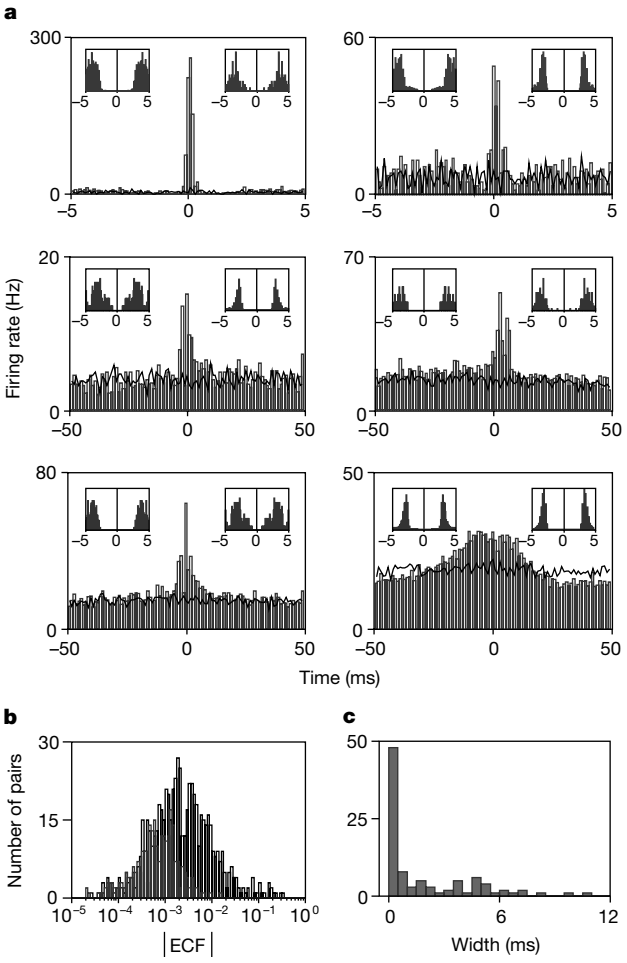


**Figure 2** The degree of correlated activity and the timescale over which it occurs. **a**, Cross-correlograms for pairs of ganglion cells. A cross-correlogram gives the firing rate of one cell relative to spikes generated by the other. Grey, the raw cross-correlogram; black, the shifted cross-correlogram (shift-predictor[14]). The latter gives the correlations produced only by the stimulus, and is generated by presenting the stimulus multiple times and cross-correlating the responses of the cells when they 'saw' the stimulus at different times. Cells are correlated if there is a peak in the raw cross-correlogram relative to the shifted. Note the expanded time scale in the top two plots. Insets, autocorrelograms for the cells in each pair; vertical axis is scaled to the height of the side peaks. **b**, Distribution of ECFs for all cell pairs. Black, pairs with positive ECFs; grey, pairs with negative ECFs. **c**, Distribution of correlation timescales, as measured by the width of the cross-correlogram, for cell pairs with ECFs above 0.5%. Widths were computed by fitting the difference between the raw and shifted cross-correlograms to a gaussian (see Supplementary Information). Characteristics of pairs of cells in **a**: top left, ON-type cells, ECF = 10.4%, $1-\Delta I/I$ = 92.4% (Fig. 3); top right, OFF-type cells, ECF = 1.8%, $1-\Delta I/I$ = 98.4%; middle left, OFF-type cells, ECF = 0.8%, $1-\Delta I/I$ = 97.8%; middle right, OFF-type cells, ECF = 4%, $1-\Delta I/I$ = 91.5%; bottom left, OFF-type cells, ECF = 1.4%, $1-\Delta I/I$ = 94.1%; bottom right, OFF-type cells, ECF = 0.8%, $1-\Delta I/I$ = 92.2%.

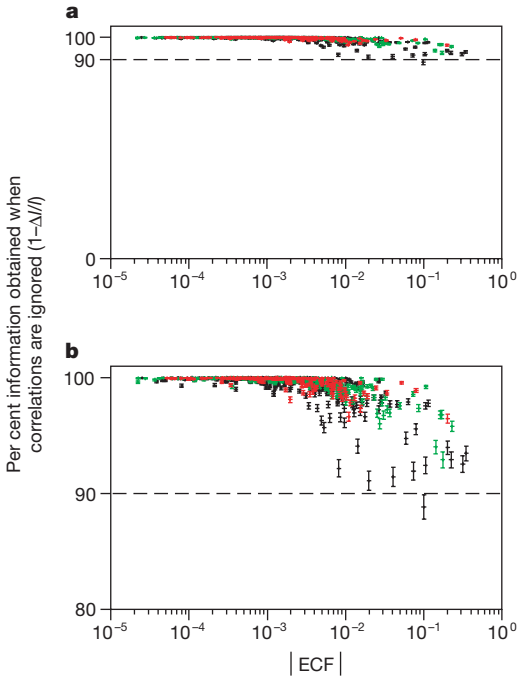


**Figure 3** Per cent of information about the stimuli obtained from ganglion cell pairs when their correlated spikes were ignored, $1-\Delta I/I$. **a**, For each pair, $1-\Delta I/I$ was plotted against the pair's ECF. All but one pair was above the dashed line at 90%, indicating that, for nearly all pairs, > 90% of the information about the stimulus was obtained when correlations were ignored. Black, red and green correspond to Movies 1, 2, and 3, respectively. (Movie 1: 444 pairs from 5 retinas; Movie 2: 229 pairs from 3 retinas; Movie 3: 263 pairs from 3 retinas. Note that a single retina viewed multiple movies.) **b**, Expanded view.

To test the reliability of our results, we checked whether cell pairs with high ECFs were somehow anomalous. If, for example, the cells in these pairs had unusually low information rates, then the measures of $\Delta I$ might be unreliable. Similarly, if there were a large discrepancy in the information between the two cells in each pair, then the measures of $\Delta I$ might also be unreliable. For example, if one cell in the pair carried most of the information, then $\Delta I$ would be small, but reflect nothing about the importance (or lack of importance) of correlations. We tested these possibilities by measuring the information rates of both cells in all pairs and by computing the ratio of the two. No trend towards low information rates was observed for pairs of cells with high ECFs ($P > 0.3$, $t$-test, comparison of cell pairs above and below 0.5% ECF), and no trend towards high ratios was found ($P > 0.6$, $t$-test, comparison of cell pairs above and below 0.5% ECF). Finally, we measured the information rates for all cells in the dataset. These ranged from 0.15 to 4.4 bits per spike, or 0.5 to 41.2 bits per s. Compared to cat LGN, the closest mammalian data available, the rates in our dataset were very similar in bits per spike, but a factor of two lower in bits per s (ref. 18). The lower rate is probably due to lower firing rates in our recordings.

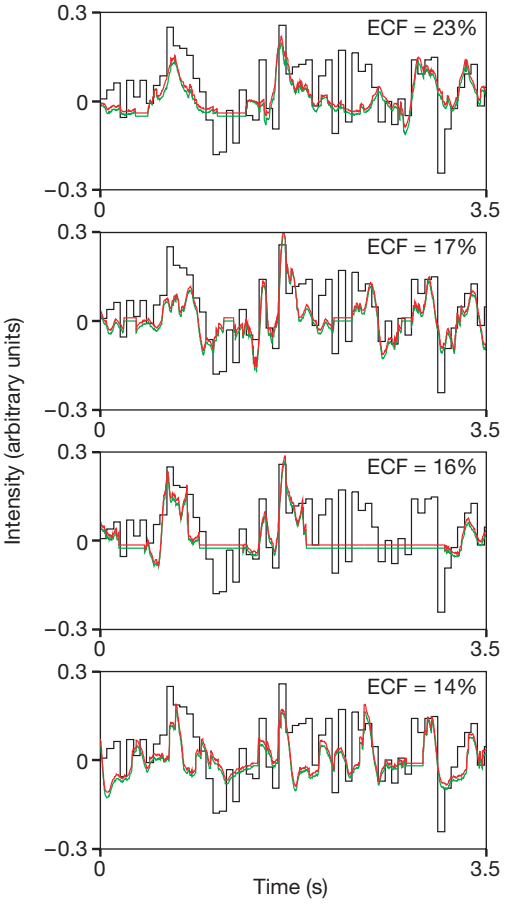


**Figure 4** Decoding ganglion cell responses two ways: when the responses were treated as independent, and when correlations in the responses were taken into account. We presented the retina with a stimulus, a spatially uniform field that varied in intensity as a function of time (Movie 3), and recorded responses from pairs of cells. We then applied a widely used decoding algorithm, linear reconstruction[26], to reconstruct the stimulus from the responses (see Supplementary Information). We performed the reconstructions on the four pairs of cells with the highest ECFs to this stimulus. Each panel shows the reconstructions for one pair. Black trace, stimulus; red trace, reconstruction of the stimulus when the responses were treated as independent; green trace, reconstruction of the stimulus when correlations were taken into account. (The red trace is shifted up by one line width so that both traces can be seen.) In all cases, the reconstruction when the responses were treated as independent was essentially the same as that when correlations were taken into account: the root mean square error between the stimulus and the two types of reconstruction differed by $< 1\%$.

Our results indicate that little information is lost when the correlated firing of retinal ganglion cells is ignored. This has direct bearing on the strategies that can be used for decoding ganglion cell activity. It indicates that strategies that treat the cells as independent encoders are reasonable, as they can capture more than 90% of the information that the cells carry. An example is shown in Fig. 4: we compared a decoding strategy that treated the responses of the cells as independent with one that took correlations in the responses into account, and found that both strategies performed essentially identically.

Our results also have practical implications. If ganglion cells can be treated as independent, then the activity of any given cell can be evaluated separately from other cells. If the cells cannot be treated as independent, then the activity of any given cell cannot be evaluated without taking into account other cells in the population. This greatly affects the amount of data needed to determine the information carried by a population of cells. If the cells are independent, then the amount of data needed scales linearly with the number of cells. If not, then the amount of data needed scales quadratically at best, and exponentially at worst, with the number of cells, making the problem data-limited and computationally intractable for more than a small number of cells. Our finding that ganglion cells act largely as independent encoders is thus significant from a practical, as well as scientific, point of view—it indicates that the problem of decoding population activity can be significantly simplified.

One caveat is that capturing more than 90% of the information in ganglion cell activity may ultimately not be enough. However, as our understanding of how populations of ganglion cells encode visual information is in its early stages, focusing on the part of the activity that carries most of the information seems a reasonable place to start.

The experiments in this study were performed in the light-adapted state of the retina (in daylight vision; see Methods). Further studies will be needed to determine whether correlated activity is important in the dark-adapted state, as the strategy for encoding information in the two states may not be the same. □

## Methods

### Definition of correlated activity

'Correlated' is defined here as a lack of independence on a stimulus-by-stimulus basis. Two neurons are correlated if their conditional probabilities are not independent; that is, if $P(r_1, r_2|s) \neq P(r_1|s)P(r_2|s)$ for at least one stimulus, $s$. Here $r_1$ and $r_2$ are the responses of cells 1 and 2, and $P(r|s)$ denotes the conditional probability of observing response $r$ given stimulus $s$.

### Stimuli

Three movies were used. Movies 1 and 2 contained scenes of male and female mice interacting. Second order spatial statistics were computed for these movies[19]; Movies 1 and 2 had $1/f^2$ and $1/f^{2.4}$ power spectra, respectively, where $f$ is spatial frequency. These are similar to the spectra of natural scenes; stills photographed in the woods exhibit a $1/f^{1.8}$ power spectra. Movie 3 had no spatial structure, but was time-varying, with a $1/\omega$ power spectrum where $\omega$ is temporal frequency.

Mean stimulus intensity was 1,050 rod-equivalent-photons per $\mu m^2$ per s. This corresponds to 500 photoisomerizations (R*) per rod per s, assuming that the mouse rod has an optical density at peak absorption wavelength of 0.011 $\mu m^{-1}$, a length of 24 $\mu$m, a diameter of 1.4 $\mu$m and a quantum efficiency of 0.67 (refs 20, 21). This stimulus intensity is in the cone regime[22,23], with rods ~90% saturated[23]. The retina was also exposed briefly ($< 4$ min) to dim red illumination during dissection. The total equivalent photon dose during dissection was small compared to that during the stimulus: ratio of dissection to stimulus dose was 1.1% for rods and 2.7% for the longer wavelength cones (see Supplementary Information for all calculations).

### Electrophysiological recording

Recordings were made with a multi-electrode array, using recording conditions described in ref. 24. To ensure that cells with overlapping receptive fields were examined, arrays with closely spaced electrodes (25–100 $\mu$m spacing) were used. As this also increased the likelihood of recording one cell on two electrodes, the following method was used to determine whether two units were from a single cell: the receptive field of each unit was

mapped using reverse correlation to a checkerboard stimulus[25]. If the two units showed identical fields, they were considered suspect. Their spike trains were then compared to determine whether they were the same cell. Eight units showed receptive fields and spike trains identical to those of another unit (>90% identical spikes). These were discarded. Three units showed receptive fields that were identical to those of another, but failed to show identical spike trains. These were retained.

### Computing the ECF

The ECF was calculated as follows: first, the raw fraction of correlated spikes for each pair was determined. This was the number of spikes that occurred within 1 ms of each other divided by the total number of spikes fired by the pair. Next, the shifted fraction was determined. This was the fraction that would have occurred by chance, taking into account correlations induced by the stimulus. It was obtained by pairing responses from the two cells when they 'saw' the stimulus at different times; that is, by pairing the response of one cell with the response of the other shifted by one movie length (the stimulus consisted of a movie repeated multiple times). We determined the shifted fraction by counting the number of spikes in the shifted pair that occurred within 1 ms of each other and dividing this by the total number of spikes for the pair. The ECF is the difference between the raw and shifted fraction.

### Computing information

$I$ and $\Delta I$ were computed as described[16]. A detailed description, including calculation of the error bars and demonstration that our estimate of $\Delta I/I$ is accurate, is given in Supplementary Information.

### Derivation of equation (2)

Information about a stimulus can be thought of as the average number of yes/no questions it would take to identify a stimulus minus the average number of yes/no questions it would take to identify the stimulus given that responses have been observed (assuming one uses the optimal question-asking strategy; see ref. 17, chapter 5). To use the optimal strategy, one needs to know the true conditional probability distribution, $P(r_1, r_2|s)$. When we treat the cells as independent, we use an approximate conditional probability distribution, $P_{\mathrm{IND}}(r_1, r_2|s)$. This leads to a less-than-optimal question-asking strategy, and thus a loss of information. The average number of yes/no questions needed to determine the stimulus given the responses using $P_{\mathrm{IND}}(r_1, r_2|s)$ is $H(S|R_1, R_2) + D(P(s|r_1, r_2)||P_{\mathrm{IND}}(s|r_1, r_2))$, where $H(S|R_1, R_2) = -\Sigma_{r_1,r_2} P(r_1, r_2)\Sigma_s P(s|r_1, r_2)\log_2 P(s|r_1, r_2)$ is the conditional entropy, and $D(P(s|r_1, r_2)||P_{\mathrm{IND}}(s|r_1, r_2)) = \Sigma_{r_1,r_2} P(r_1, r_2)\Sigma_s P(s|r_1, r_2)\log_2[P(s|r_1, r_2)/P_{\mathrm{IND}}(s|r_1, r_2)]$ is the conditional relative entropy (see ref. 17, theorem 5.4.3, p.89). The distributions $P(s|r_1, r_2)$ and $P_{\mathrm{IND}}(s|r_1, r_2)$ come from $P(r_1, r_2|s)$ and $P_{\mathrm{IND}}(r_1, r_2|s)$ via Bayes' theorem. Using the standard result that the average number of yes/no questions needed to determine the stimulus when no responses have been observed is simply $H(S)$, the entropy of the stimulus[17], we find that the difference, $\Delta I$, between the information given by the true distribution and that given by the approximate distribution is $\Delta I = D(P(s|r_1, r_2)||P_{\mathrm{IND}}(s|r_1, r_2))$, in bits. Bayes' theorem reduces this expression to equation (2).

Received 29 February; accepted 12 April 2001.


1. Gray, C. M. The temporal correlation hypothesis of visual feature integration: still alive and well. *Neuron* **24,** 31–47 (1999).
2. Shadlen, M. N. & Movshon, J. A. Synchrony unbound: a critical evaluation of the temporal binding hypothesis. *Neuron* **24,** 67–77 (1999).
3. Panzeri, S., Schultz, S. R., Treves, A. & Rolls, E. T. Correlations and the encoding of information in the nervous system. *Proc. R. Soc. Lond. B* **266,** 1001–1012 (1999).
4. Nirenberg, S. & Latham, P. E. Population coding in the retina. *Curr. Opin. Neurobiol.* **8,** 488–493 (1998).
5. Meister, M. Multineuronal codes in retinal signaling. *Proc. Natl Acad. Sci. USA* **93,** 609–614 (1996).
6. Meister, M., Lagnado, L. & Baylor, D. A. Concerted signaling by retinal ganglion cells. *Science* **270,** 1207–1210 (1995).
7. Warland, D. K., Reinagel, P. & Meister, M. Decoding visual information from a population of retinal ganglion cells. *J. Neurophysiol.* **78,** 2336–2350 (1997).
8. Rodieck, R. W. Maintained activity of cat retinal ganglion cells. *J. Neurophysiol.* **30,** 1043–1071 (1967).
9. Mastronarde, D. N. Correlated firing of cat retinal ganglion cells. I. Spontaneously active inputs to X- and Y-cells. *J. Neurophysiol.* **49,** 303–324 (1983).
10. Mastronarde, D. N. Correlated firing of cat retinal ganglion cells. II. Responses of X- and Y-cells to single quantal events. *J. Neurophysiol.* **49,** 325–349 (1983).
11. Devries, S. H. Correlated firing in rabbit retinal ganglion cells. *J. Neurophysiol.* **81,** 908–920 (1999).
12. Chichilnisky, E. J. & Baylor, D. A. Synchronized firing by ganglion cells in monkey retina. *Soc. Neurosci. Abstr.* **25,** 1042 (1999).
13. Alonso, J. M., Usrey, W. M. & Reid, R. C. Precisely correlated firing in cells of the lateral geniculate nucleus. *Nature* **383,** 815–819 (1996).
14. Perkel, D. H., Gerstein, G. L. & Moore, G. P. Neuronal spike trains and stochastic point processes. II. Simultaneous spike trains. *Biophys. J.* **7,** 419–440 (1967).
15. Shannon, C. E. & Weaver, W. *The Mathematical Theory of Communication* (Univ. Illinois Press, Urbana, Illinois, 1949).
16. Strong, S. P., Koberle, R., de Ruyter van Steveninck, R. R. & Bialek, W. Entropy and information in neural spike trains. *Phys. Rev. Lett.* **80,** 197–200 (1998).
17. Cover, T. M. & Thomas, J. A. *Elements of Information Theory* (Wiley, New York, 1991).
18. Reinagel, P. & Reid, R. C. Temporal coding of visual information in the thalamus. *J. Neurosci.* **20,** 5392–5400 (2000).
19. Ruderman, D. L. & Bialek, W. Statistics of natural images: Scaling in the woods. *Phys. Rev. Lett.* **73,** 814–817 (1994).
20. Carter-Dawson, L. D. & LaVail, M. M. Rods and cones in the mouse retina. I. Structural analysis using lights and electron microscopy. *J. Comp. Neurol.* **188,** 245–262 (1979).
21. Penn, J. S. & Williams, T. P. A new microspectrophotometric method for measuring absorbance of rat photoreceptors. *Vision Res.* **24,** 1673–1676 (1984).
22. Soucy, E., Wang, Y., Nirenberg, S., Nathans, J. & Meister, M. A novel signaling pathway from rod photoreceptors to ganglion cells in mammalian retina. *Neuron* **21,** 481–493 (1998).
23. Dodd, R. L. in *Program in Neurosciences* 153–156 (Stanford Univ., Palo Alto, 1988).
24. Nirenberg, S. & Meister, M. The light response of retinal ganglion cells is truncated by a displaced amacrine circuit. *Neuron* **18,** 637–650 (1997).
25. Meister, M., Pine, J. & Baylor, D. A. Multi-neuronal signals from the retina: acquisition and analysis. *J. Neurosci. Methods* **51,** 95–106 (1994).
26. Bialek, W., Rieke, F., de Ruyter van Steveninck, R. R. & Warland, D. Reading a neural code. *Science* **252,** 1854–1857 (1991).


**Supplementary information** is available on *Nature*'s World-Wide Web site (http://www.nature.com) or as paper copy from the London editorial office of *Nature*.


### Acknowledgements

We thank J. Assad, A. Pouget, T. Otis, D. Buonomano and M. Goldman for critical reviews of the manuscript. We also thank M. Jack, J. Sinclair, F. Schweizer, J. Feldman and M. Meister for helpful discussion. This work was supported by grants from the Beckman Foundation and the Klingenstein Fund (S.N.).


Correspondence and requests for materials should be addressed to S.N. (e-mail: sheilan@ucla.edu).

# Regulation of $Ca^{2+}$ channel expression at the cell surface by the small G-protein kir/Gem


**Pascal Béguin*†‡, Kazuaki Nagashima*‡, Tohru Gonoi§, Tadao Shibasaki*, Kazuo Takahashi‖, Yasushige Kashima*, Nobuaki Ozaki*, Käthi Geering†, Toshihiko Iwanaga¶ & Susumu Seino***

** Department of Cellular and Molecular Medicine, Graduate School of Medicine, Chiba University, 1-8-1 Inohana, Chuo-ku, Chiba 260-8670, Japan*
*† Institut de Pharmacologie et de Toxicologie de l'Université de Lausanne, 27 rue du Bugnon, CH-1005 Lausanne, Switzerland*
*§ Research Center for Pathogenic Fungi and Microbial Toxicoses, Chiba University, 1-8-1, Inohana, Chuo-ku, Chiba 260-8673, Japan*
*‖ Department of Molecular Immunology, Core Research for Evolutional Science and Technology (CREST), Graduate School of Medicine, Chiba University, 1-8-1 Inohana, Chuo-ku, Chiba 260-8670, Japan*
*¶ Laboratory of Anatomy, Graduate School of Veterinary Medicine, Hokkaido University, Sapporo 060-0818, Japan*
*‡ These authors contributed equally to this work.*



**Voltage-dependent calcium ($Ca^{2+}$) channels are involved in many specialized cellular functions[1–3], and are controlled by intracellular signals such as heterotrimeric G-proteins[4], protein kinases[5,6] and calmodulin (CaM)[7,8]. However, the direct role of small G-proteins in the regulation of $Ca^{2+}$ channels is unclear. We report here that the GTP-bound form of kir/Gem, identified originally as a Ras-related small G-protein that binds CaM[9–11], inhibits high-voltage-activated $Ca^{2+}$ channel activities by interacting directly with the β-subunit. The reduced channel activities are due to a decrease in $\alpha_1$-subunit expression at the plasma membrane. The binding of $Ca^{2+}$/CaM to kir/Gem is required for this inhibitory effect by promoting the cytoplasmic localization of kir/Gem. Inhibition of L-type $Ca^{2+}$ channels by kir/Gem prevents $Ca^{2+}$-triggered exocytosis in hormone-secreting cells. We propose that the small G-protein kir/Gem, interacting with β-subunits, regulates $Ca^{2+}$ channel expression at the cell surface.**


The $\alpha_1$1.2- and $\alpha_1$1.3-subunits of L-type $Ca^{2+}$ channels (formerly termed $\alpha_{1C}$ and $\alpha_{1D}$, respectively[12]) are associated with auxiliary subunits (β-, $\alpha_2\delta$- and γ-subunits) that have regulatory functions[13].